Drying Kinetics of Polymer Films

Béatrice Guerrier, Charles Bouchard, Catherine Allain, and Christine Bénard
Lab. FAST, CNRS—Université Pierre et Marie Curie—Université Paris Sud, 91405 Orsay, France

Drying kinetics of a polymer film cast from a polymer–solvent solution is studied. A modelization of the whole drying process is performed, including the diffusion of solvent through the varnish layer, the moving interface, and the coupled heat and mass transfer between the interface and the drying air. The assumptions and the validity domain of the proposed modelization are thoroughly analyzed. In particular, comparison of the varnish temperature with its glass transition temperature all along the process allows us to determine the validity domain of the Fickian diffusion assumption. Because of the hypodiffusive behavior of polymer solutions, very large concentration gradients appear in the layer, and the drying kinetics is characterized by two successive regimes. This two-stage kinetics is investigated first for typical conditions encountered in the packaging industry, where a film of a few microns is dried in a few seconds, thanks to hot air blown through nozzles. Then, different drying conditions corresponding to evaporation experiments at room temperature of thicker films of the same varnish are studied.

Introduction

Understanding the drying kinetics of a polymer film cast from a polymer/solvent solution is a major issue in numerous industrial processes. Indeed, most of lacquer, paint, and varnish coatings are obtained by performing solvent evaporation from an initial dilute solution (Vrentas and Vrentas, 1994). Besides coating technology, another application is the evaporation step of asymmetric membrane casting (Krantz et al., 1986). Controlling the drying rate is important, in order to minimize the residual solvent (especially in food-packaging applications) and ensure good mechanical properties. The optimization of such processes is complex, since the drying kinetics is controlled by several phenomena, and results from both operating conditions and physicochemical properties of the solution.

As known for polymer/solvent solutions, the solvent mutual diffusion coefficient decreases by several orders of magnitude when the solvent concentration decreases (Duda et al., 1979; Hwang and Cohen, 1984; Neogi, 1996). As a consequence, very large concentration gradients appear in the layer, and the drying kinetics is characterized by two successive regimes: in the first stage, the solution is still rather dilute and the solvent concentration high enough to allow an important flux of solvent up to the interface. Moreover, the solvent activity is close to one, and the evaporation flux is quite similar to the one we would get by evaporating pure solvent. The kinetics of this "fast" regime then depends strongly on the coupled heat and mass transfers between the moving interface and the air. The film thickness shrinks rapidly. In a second stage, as the solvent concentration is falling down in the upper layer near the interface, both diffusion and evaporation decrease significantly and the physicochemical properties of the solution have a determining influence on this "slow" regime.

This article deals with the description and the modelization of the whole drying of a polymer film, namely the diffusion of the solvent through the varnish layer, the moving interface, and the coupled heat and mass transfers between the interface and the drying air. The usual assumptions and equations encountered in the description of such processes can be found in some previous works (Krantz et al., 1986; Vrentas and Vrentas, 1994; Cairncross et al., 1995). Based on this description, we performed a sensitivity analysis to investigate the influence of the various process parameters on the drying kinetics in a typical industrial configuration. One of the major assumptions usually used is Fickian diffusion in the layer, that is, the possible transition from rubbery to glassy state is not taken into account. In order to reliably evaluate the validity of this assumption, an accurate numerical scheme has been developed. It yields the temperature of the layer and the concentration profile evolution up to the very end of the process. At each time, the temperature of the varnish can then be compared with its glass transition temperature.

Correspondence concerning this article should be addressed to B. Guerrier.

The drying kinetics have been investigated for two different situations: the first one corresponds to typical coating conditions in the packaging industry, where a film of a few microns is dried in a few seconds, thanks to hot air blown through a set of nozzles. The same samples have also been used to perform simple evaporation experiments, where a thicker film (a few mm) dries thanks to evaporation in room air: unlike for the industrial situation, it was then possible to record the solvent mass evolution, and to compare it with the proposed model.

The industrial process is given in Figure 1: after coating, the aluminum substrate goes through the dryer where hot air jets impinge onto the foil perpendicularly through a set of nozzles. The air charged with solvent vapor is evacuated, but may be partly recycled into the blowing circuit. No radiant heating is added in the process. The typical range of the aluminum sheet velocity is between 0.8 and 5 m/s, which corresponds to a total drying time of a few seconds. The drying air is characterized by its temperature T_a (50 to 150°C), its mean velocity in a nozzle section, v_a ($\sim$ 45 m/s), and the solvent vapor concentration $(\rho_s^g)_\infty$ (in g/m^3). The varnish is mainly composed of a mixture of several copolymers dissolved in an organic solvent. In the process considered here, no polymerization reaction takes place during the drying process, and the solid film is obtained by solvent extraction only. The initial solvent concentration is chosen according to the rheological and wetting properties: the solution viscosity, which strongly depends on the polymer concentration, must ensure good coating conditions. For the varnish considered here, the initial polymer mass fraction (ES) is about 20%.

The article is organized as follows: in the following section, the model and its underlying physical assumptions are presented, as well as the heat and mass balances, the boundary conditions, and the constitutive laws used to solve the problem. The numerical procedure is also given in that section. The third section is devoted to the analysis of the simulated drying kinetics in the industrial conditions. In particular, the influence of the drying air parameters is tested, and a validation of the rubbery state assumption is proposed. In the fourth section, we present the evaporation experiments in ambient air and the validation of the previous model.

Physical Model

Presentation

The purpose of this section is to briefly recall the various assumptions usually made for the description of such processes. For clarity, they are detailed for the industrial-dryer configuration. The few modifications needed for the other configuration (evaporation in ambient air) are given in the fourth section.

After coating, the aluminum foil enters the drying chamber, with a concentration solvent/polymer uniform throughout the whole layer thickness. Figure 2 shows the foil and the film and defines some of the notation used in the following. Because of the high rolling velocity and the geometry of the drying machine, one may assume that the main direction of heat and mass transfer in the layer and in the interface vicinity is perpendicular to the foil. In that way, the problem is reduced to only two variables, the spatial direction normal to the sheet (z) and the time (t). Then, a 1-D model is considered (cf. Figure 2).

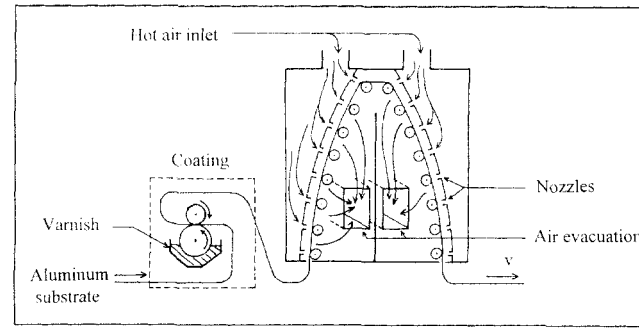

Figure 1. Coating unit and the drying chamber.

The heat and mass transfer between air and foil can be expressed thanks to overall exchange coefficients: h_{th}^{sup} and h_{th}^{inf} (W/m$^2\cdot$°C) for the heat transfer on the varnished and nonvarnished sides of the foil, respectively; and h_m (m/s) for the solvent mass transfer (cf. Figure 2). Due to the large value of the thermal diffusivity ($\simeq 10^{-7}$ m^{2}s^{-1}), that is, about one thousand times higher than the maximum value of the mass-diffusion coefficient, one can assume that the thermal diffusion time is negligible. Moreover the thermal Biot numbers, defined as $h_{th}^{sup}e/\lambda$, and $h_{th}^{inf}e/\lambda$ for the upper and lower face, respectively (where e is the thickness and λ the thermal conductivity), are lower than 5×10^{-3} due to the small thickness involved. Temperature gradients through the layer and the aluminum substrate are thus negligible, and a uniform temperature over the whole substrate and film will be considered: an element dx is characterized by a single temperature $T(t)$ that depends only on time.

During the whole drying process, the varnish temperature is supposed to be greater than the glass transition temperature, so that the solution behaves like a viscous binary mixture (rubbery state) (Vrentas et al., 1977). Under this assumption, Fickian-type diffusion is considered and the solvent flux only depends on the concentration gradient. This assumption is clearly valid at the beginning of the process, when the solvent concentration is high, since the glass transition temperature of the initially deposited solution is well below the ambient temperature. The Fickian diffusion assumption becomes more problematic when the solvent weight fraction ω_S falls to a very low value (ω_S less than 0.05) near the interface, since the glass transition temperature of a polymer

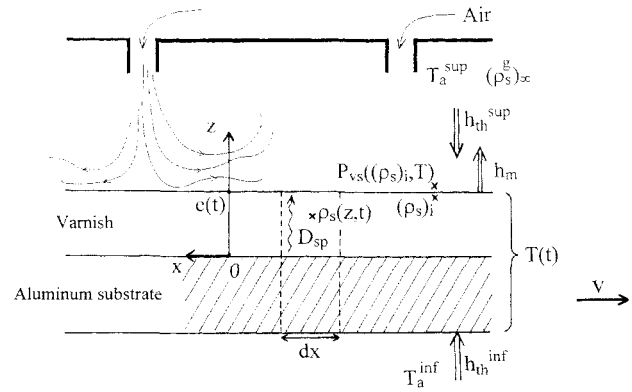

Figure 2. Drying chamber and film: 1-D model.

solution, T_g, increases very rapidly as solvent concentration decreases (Chow, 1980). As the proposed model gives both temperature and concentration profiles through the varnish as a function of time, the comparison at each time of $T(\omega_S)$ and $T_g(\omega_S)$ (where ω_S is the minimal value of the solvent weight fraction, that is, near the air/varnish interface) allows us to determine *a posteriori* whether the assumption of Fickian diffusion is valid. As seen later, for the varnish considered in this article, and for typical operating conditions, this assumption can be considered as valid during the whole process. If this was not the case, the modelization should be enlarged in order to take into account the viscoelastic behavior of the polymer solution. The problem is then more complex, and a large number of studies, both theoretical and experimental, are still devoted to the study of non-Fickian diffusion. One can refer among others to the works of (Thomas and Windle, 1982; Durning and Tabor, 1986; Gall et al., 1990; Billovits and Durning, 1993, 1994; Rossi et al., 1995; Edwards and Cohen, 1995a,b). Various approaches are proposed to take into account the plasticization effects due to the solvent: for example, they are treated by setting an upper limit to the velocity of the rubbery/glassy state front in the approach proposed by (Rossi et al., 1995), or by considering two coupled evolution equations for concentration and viscoelastic stress in order to approximate the "memory" of the polymer with respect to its history in Edwards and Cohen (1995b).

Heat and mass-transfer equations

The coupled heat and mass-transfer equations are now briefly presented. The variables considered in the following are the temperature $T(t)$ of the sheet, the local partial density of solvent $\rho_S(z,t)$, and the thickness of the layer $e(t)$.

The thermal balance is given by Eq. 1: the thermal energy brought by exchange with the ambient air is used partly to vaporize the solvent, and partly to heat the sheet:

$$\left(\rho^{al}c_p^{al}e^{al}+\overline{\rho c_p}e(t)\right)\frac{dT}{dt} = h_{th}^{\sup}(T_a^{\sup}-T)+h_{th}^{\inf}(T_a^{\inf}-T)-L_V\Phi_m, \quad (1)$$

where $\rho^{al}c_p^{al}e^{al}$ is the substrate thermal capacity per unit area of sheet (J/m^2 °C), $\overline{\rho c_p}e(t)$ is the varnish thermal capacity, which is estimated as an average over the whole thickness of varnish, using the intrinsic specific heats of polymer and solvent. L_V and Φ_m are the vaporization heat (J/g) and the evaporating solvent flux (g/m^2·s), respectively. The latter is given by the following:

$$\Phi_m = h_m\left[\frac{(P_{VS})_{\text{interface}}M_S}{RT}-(\rho_S^g)_\infty\right], \quad (2)$$

where $(P_{VS})_{\text{interface}}$ is the saturating vapor pressure of the polymer/solvent mixture under consideration, taken at the current sheet's temperature and at the solvent concentration in the varnish near the interface ($z=e(t)$), M_S is the solvent molar mass, R the gaz constant, and $(\rho_S^g)_\infty$ is the solvent vapor concentration in air far from the film/air interface. Let us emphasize that heat and mass transfers are coupled through P_{VS}, which is a function of both temperature and solvent volume fraction φ_S: $(P_{VS})_{\text{interface}} = P_{VS}[T(t),\ \varphi_S(t, z=e(t))]$. The saturating vapor pressure is one of the key parameters of this coupled problem.

The local solvent partial density $\rho_S[t, z=e(t)]$ results from the modelization of the diffusive mass transfer throughout the varnish layer. In the spatial domain $[0;\ e(t)]$, the local conservation of the solvent expresses as (Bird et al., 1960)

$$\frac{\partial\rho_S}{\partial t}-\frac{\partial}{\partial z}\left(D_{SP}(\omega_S,T)\frac{\partial\rho_S}{\partial z}\right)=0 \quad (3)$$

Due to the large dependence of the mutual diffusion coefficient D_{SP} vs. the temperature T and, above all, vs. solvent weight fraction ω_S, Eq. 3 is strongly nonlinear. The initial conditions for the differential Eqs. 1 and 3 are: $T(t=0)=T_0$; $\rho_S(z,t=0)=\rho_{S_0}$; $e(t=0)=e_0$.

The boundary conditions are

- At $z=0$: the solvent mass flux equals zero since the substrate is impermeable, hence: $[\partial\rho_S/\partial z]_{z=0}=0$.
- At $z=e(t)$: the continuity of solvent mass flux across the interface gives

$$\left[-\rho_S\frac{de}{dt}-D_{SP}(\omega_S,T)\frac{\partial\rho_S}{\partial z}\right]_{z=e(t)}=\Phi_m. \quad (4)$$

The motion of the varnish/air interface, due to solvent evaporation, is taken into account through the term de/dt (Caroli et al., 1992).

Another equation is obtained by writing the impermeability of the varnish/air interface to polymers (polymers do not evaporate):

$$\frac{de}{dt}=-V_S\,\Phi_m. \quad (5)$$

Dimensionless variables and numerical procedure

We solved the equation set numerically using the following dimensionless variables:

$$\tau=(tD_{SP_0})/e_0^2, \qquad Z=z/e_0, \qquad \eta=e/e_0$$

$$\psi=\rho_S/\rho_{S_0}, \qquad \psi_\infty^g=(RT/M_SP_{VS_0}(T_0))(\rho_S^g)_\infty$$

$$\theta=(T-T_0)/(T_a^{\sup}-T_0)$$

$$D_{SP}^*=D_{SP}/D_{SP_0}, \qquad P_{VS}^*=P_{VS}/P_{VS_0}(T_0),$$

where D_{SP_0} is the value of D_{SP} for $\omega_S\to 1$ and P_{VS_0} is the saturating vapor pressure of the pure solvent that is a known function of T only.

The numerical resolution of this problem raises some specific difficulties:

- The diffusion equation (Eq. 3) is strongly nonlinear because of $D_{SP}(\omega_S,T)$.
- Heat and mass transfer are coupled through $P_{VS}(\varphi_S,T)$ and $D_{SP}(\omega_S,T)$.
- Boundary condition 4 induces a coupling with the actual solvent concentration at the interface that results from the whole preceding drying kinetics.

• The interface velocity is very large. This moving boundary was handled using the Landau transformation (Crank 1988): the physical moving domain is mapped onto a fixed domain by the following coordinate transformation: $Y = Z/\eta$. Thanks to this transformation, the spatial grid has not to be modified during the simulation, but the transformation generates a pseudoconvective term in the diffusion equation, proportional to the interface velocity $\dot{\eta}$:

$$\frac{\partial \psi}{\partial \tau} - Y\dot{\eta}/\eta \frac{\partial \psi}{\partial Y} - 1/\eta^2 \frac{\partial}{\partial Y}\left(D^*_{SP} \frac{\partial \psi}{\partial Y} \right) = 0. \qquad (6)$$

The transformed equations are then discretized using a finite volume method. Concerning the resolution algorithm, we solve at each time step the diffusion equation using the values of D_{SP}, temperature, Neumann boundary condition 4 and interface velocity—required in the pseudoconvective term in Eq. 6—coming from the previous time step or iteration. Iterations on D_{SP} are first achieved until convergence of Eq. 6; then iterations on the other coupling variables are also achieved.

Since an important concentration gradient appears near the interface, and since the diffusion coefficient decreases very strongly with solvent concentration, a very precise space discretization is needed in order to ensure the numerical convergence of the iterative procedure. For some of the results presented in the following, the thickness of the first finite volume (near the interface) has to be reduced down to 2.5×10^{-5} (dimensionless value in the fixed domain of thickness = 1). In order to limit the total number of finite volumes, an irregular grid was used, based on a geometrical progression. With a progression rate of about 1.04, 200 grid points are needed. The dimensionless time step was 3×10^{-7}. Tests are performed during the whole simulation to ensure that the two usual criteria, $C_1 = D_{SP}\delta t/(\delta z)^2$ and $C_2 = \dot{e}\delta t/(\delta z)$, are sufficiently small.

Kinetics Analysis: Industrial Configuration

Choice of the parameters

As seen through the presentation of the physical model, the simulation of the drying kinetics needs on the one hand some parameters characterizing the operating conditions, namely the exchange coefficients, and on the other hand some physicochemical properties of the polymer solution, among which are the saturating vapor pressure and the diffusion coefficient.

Exchange Coefficients. The transfer coefficients h_{th}^{sup} and h_m, corresponding to the blowing of air onto the sheet through a set of nozzles, depend on the velocity of air (v_a) at the exit of the nozzles, on the nozzles geometry, and on the thermophysical properties of air with solvent vapor. To get an estimation of these coefficients, the following procedure has been used: a first estimation was made from various experimental studies available in the literature for similar geometries (Gardon and Akfirat, 1966; Martin, 1977). Note that the radiative contribution is negligible with regard to the convective heat exchange by blowing. The estimation of h_{th}^{inf} takes into account the heat exchange by air flow as well as the radiative transfer and the conductive transfer by contact with the rollers. These estimations were then confirmed thanks to experimental measurements of air temperature, air velocity, and foil temperature at the oven exit, performed on an industrial dryer. Finally, considering all the uncertainties, we get (Benard et al., 1994) $h_{th}^{sup} = 150 \pm 40$ W/m$^2\cdot$°C, $h_{th}^{inf} = 25 \pm 15$ W/m$^2\cdot$°C, $h_m = 0.1 \pm 0.05$ m/s.

Varnish Properties.

1. Diffusion coefficient. Numerous studies have been devoted to the analysis of diffusion in polymer solutions. Depending on the concentration domain, several theoretical approaches have been proposed (Waggoner et al., 1993), among them the framework of the scaling laws for semidilute solutions (DeGennes, 1979), and the free-volume theory for the self-diffusion in concentrated solutions (Vrentas et al., 1985). No general relationship between self- and mutual-diffusion coefficients is currently available, though some approximated relations have been developed (Duda et al., 1979; Neogi, 1996). Thus it is difficult to take advantage of these results to get an analytical expression of the mutual diffusion coefficient for the whole concentration domain ($0.8 > \omega_S > 0$) under consideration. Moreover, the varnish studied is a complex mixture of copolymers, and the physical parameters needed, for example, in the free-volume theory, are not available. That is why we have chosen to use experimental data obtained by Hwang and Cohen (1984) for the system methyl ethyl ketone (MEK), poly butyl methacrylate (PBMA), which is somewhat analogous with the industrial products under consideration. Figure 3 gives the values measured for different polymer mass fractions. For ω_s smaller than 0.3, it appears that D_{sp} declines dramatically by more than two orders of magnitude. The last point [$\log(D_{SP}) \simeq -12.5$ for $\omega_S = 0$] is an extrapolated point, since it is very difficult to obtain (both theoretically and experimentally) the diffusion coefficient at a very weak solvent concentration.

These experimental values have been obtained at about 20°C. Under the assumption of a rubbery state ($T > T_g$), an Arrhenius expression can be used to describe the dependence of D_{SP} with temperature, but with an apparent activation energy that increases by a significant amount with polymer concentration (Blum and Pickup, 1987; Lodge et al., 1990). Due to the lack of data for the studied products, we

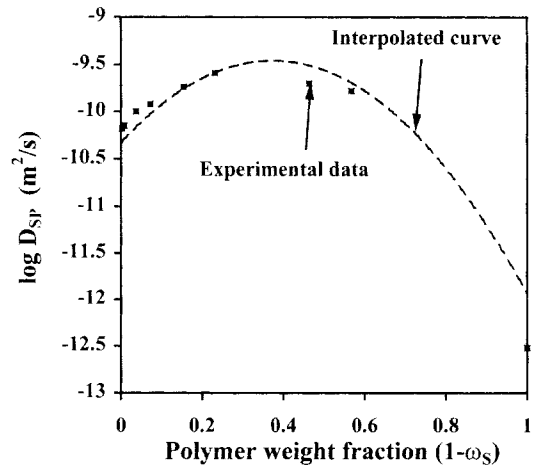

Figure 3. Mutual diffusion coefficient vs. polymer weight fraction: experimental data for MEK/PBMA (Hwang and Cohen, 1984) and interpolation used in the simulation (dashed line).

have chosen to take into account the dependence of D_{SP} with temperature in a simplified way: for the industrial configuration studied, it will be seen that the varnish temperature increases up to 100°C at the end of the process, when solvent concentration falls to very small values. Then, we have attenuated the decrease of D_{SP} for $\omega_P > 0.9$ (i.e., $\omega_S < 0.1$), setting: $\log(D_{SP}) \simeq -12$ for $\omega_S = 0$ instead of $\log(D_{SP}) \simeq -12.5$. (This would correspond to an apparent activation energy of about 13 kJ/mol for $\omega_S = 0$.) The corresponding numerical interpolation used in this section to perform the drying simulation is shown in Figure 3 (dashed line). This empirical law was shown to yield the good order of magnitude of the solvent residual mass obtained at the end of the drying, in regard to the industrial measurements. Indeed, the relative difference $(m_{simu} - m_{meas})/m_{meas}$ (where m_{meas} is the measured solvent mass and m_{simu} the simulated one) lies between 1 and 5, which is several orders of magnitude lower than the overall solvent mass variation during the whole process.

2. Saturating vapor pressure. The classic Flory–Huggins relation (Flory, 1953) was used to express the variation of P_{VS} with solvent concentration, according to the assumption that the film remains in the rubbery state (Berens, 1989; Leibler and Sekimoto, 1993):

$$P_{VS} = P_{VS_0}(T)\ \rho_S V_S \exp\left[1 - \rho_S V_S + \chi(1 - \rho_S V_S)^2\right] \quad (7)$$

where $P_{VS_0}(T)$ is known for the solvent MEK; $\rho_S V_S = \varphi_S$ is the solvent volume fraction; and χ is the Flory–Huggins coefficient. It quantifies the mutual affinity between polymer and solvent. Since χ values are missing for our two copolymer industrial varnish, we took $\chi = 0$, which corresponds to a "good solvent." In the following, it is shown that the influence of the χ parameter on the drying kinetics is small. The other physical constants needed to perform the simulation can easily be found in the literature (Brandrup and Immergut, 1989).

Analysis of the process kinetics

The results given below have been obtained with the following parameters: $T_a = 100$°C, $h_{th}^{sup} = 150$ W/m^2·°C, $h_{th}^{inf} = 25$ W/m^2·°C, $h_m = 0.05$ m/s, $(\rho g)_\infty = 0$, $T_0 = 20$°C, $ES = 0.2$, $\chi = 0$.

The time evolution of the solvent mass during the drying process is given in Figure 4, while Figure 5 shows the solvent weight fraction profile in the layer at different times. Note that the temperature conditions are such that the solvent vapor pressure does not rise above the atmospheric pressure, that is, no bubbling occurs unlike in Cairncross et al. (1995). As can be seen, the drying kinetics is characterized by two distinct regimes: in the first part (t less than about 0.45 s), the solvent mass decreases very rapidly. During this "fast" regime, the solvent weight fraction at the air/film interface remains greater than 0.25. Both the solvent activity and the diffusion coefficient are still quite high ($P_{VS}/P_{VS_0} \geq 0.65$ and $D_{SP} \geq 4.5 \times 10^{-11}$ m^2·s^{-1}), so that important diffusion and evaporation fluxes take place. In the second part ($t > 0.45$ s), however, as the diffusion coefficient decreases significantly for solvent weight fraction smaller than 0.25 (cf. Figure 3),

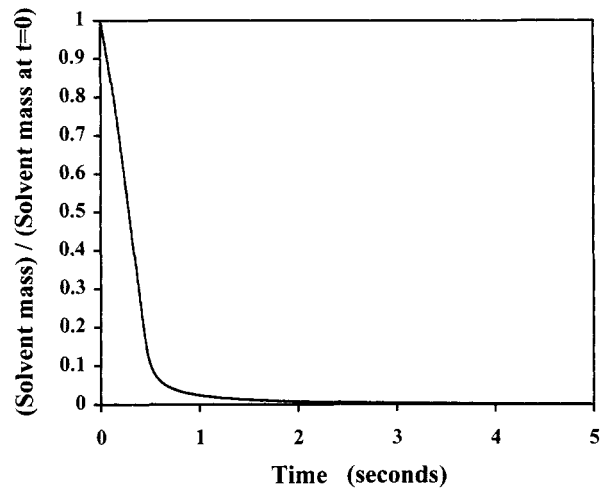

Figure 4. Solvent mass evolution during the drying process.

diffusion becomes too slow to allow a sufficient regeneration of solvent near the interface. As a consequence, a very large concentration gradient appears near the interface (cf. Figure 5). The decrease of the solvent concentration near the interface results in a decrease of the partial pressure vapor. Both coupled phenomena lead to the kinetics and profile evolution shown in Figures 4 and 5. As the drying goes on ($t > 0.5$ s), the evaporation flux becomes very weak and the concentration gradient relaxes slowly.

The thermal behavior is illustrated in Figure 6. In the first regime, the varnish temperature increases slowly, since the thermal energy brought by exchange with the ambient air is mainly used to vaporize the solvent. After the transition, the evaporation flux becomes very small, and the temperature increases toward the air temperature. The evolution of the temperature vs. the solvent mass fraction near the interface is given in Figure 7, together with the glass transition temperature. The glass transition temperature of the dry varnish ($\omega_S = 0$) was obtained by differential scanning calorimetry, and the decrease of T_g with solvent concentration was estimated

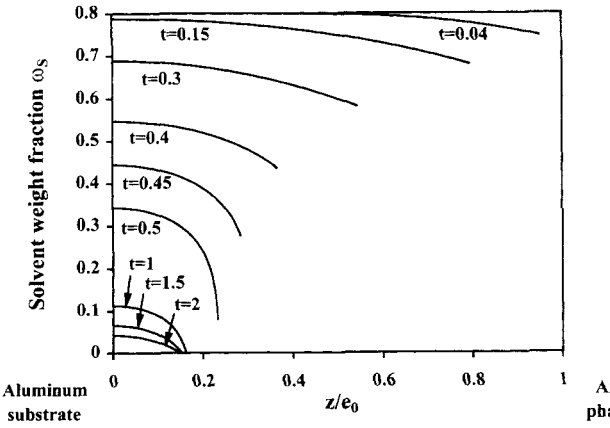

Figure 5. Solvent weight-fraction profiles in the varnish film, at various times (in seconds), corresponding to the "fast" regime ($t \leq 0.45$ s) and to the "slow" regime ($t > 0.45$ s).

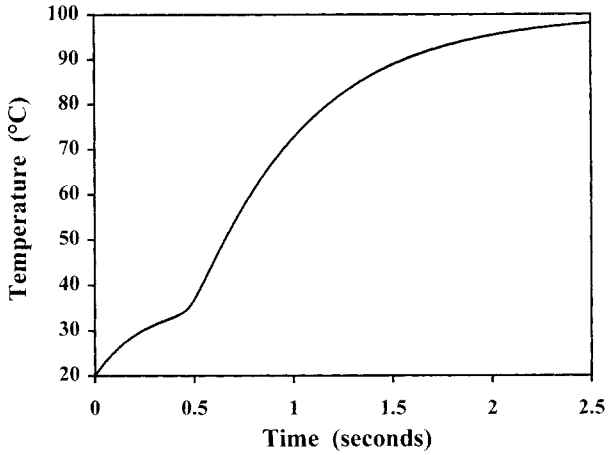

Figure 6. Film-temperature evolution.

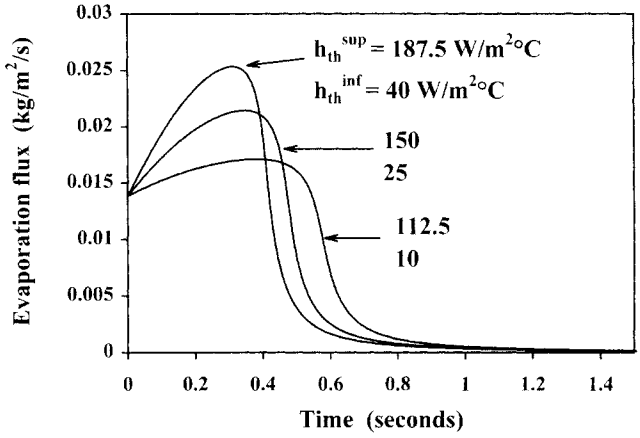

Figure 8. Influence of exchange coefficients on the drying kinetics.

thanks to the expression given in Chow (1980). As seen in this figure, the assumption "$T \geq T_g$" used to perform the simulation is validated *a posteriori*, and the layer may be considered in a rubbery state all along the drying, at least in the first approximation.

The evolution of the evaporation flux Φ_m (Eq. 2) during the process (Figure 8) shows again the coupled influence of temperature and concentration for given values of h_{th}^{sup} and h_{th}^{inf}. In the beginning, Φ_m grows due to the change of P_{VS} under increasing temperature, then Φ_m decreases since the dependence of P_{VS} on concentration becomes preponderant. To estimate the influence of the interaction parameter χ, we also computed the evolution of P_{VS} for $\chi = 0.5$. Let us recall that $\chi = 0.5$ corresponds to a lower solubility than the parameter $\chi = 0$ used previously. As a consequence, the evaporation is easier, so that the maximal value of P_{VS} is about 120 mm Hg (16×10^3 Pa) instead of 115 mm Hg (15.3×10^3 Pa) for $\chi = 0$. For $t = 2.5$ s, corresponding to the second regime, the relative difference on the residual mass is less than 2%, which is low in regard to the influence of the other parameters.

Influence of drying air parameters

The objective of this section is to analyze the influence of the drying air characteristics, within their usual variation range. The influence of air velocity is taken into account through the exchange coefficients. Different values of these coefficients, in their validity domain defined in the subsection titled "Choice of Parameters," have been considered. The corresponding evaporation fluxes are given in Figure 8. The influence of the exchange coefficients is important at the beginning, in the first regime. Concerning the residual mass at $t = 2.5$ s, that is, long after the first regime, the relative difference is less than $\pm 10\%$. Similar results are obtained by varying the air temperature between $T_a = 75$ and 125°C.

We can also compare the solvent mass evolution for $(\rho_S^g)_\infty = 0$, 10^{-2}, and 5×10^{-2} kg/m^3 (for safety reasons, $(\rho_S^g)_\infty$ is kept much below 5×10^{-2} kg/m^3). The air recycling rate influences $(\rho_S^g)_\infty$ during the process. The presence of a small amount of solvent in the drying air does not significantly affect the kinetics: the duration of the evaporation regime remains almost unchanged, and the increase of the solvent residual mass at $t = 2.5$ s is only about 15% for the extreme value $(\rho_S^g)_\infty = 5 \times 10^{-2}$ kg/m^3 in regard to $(\rho_S^g)_\infty = 0$.

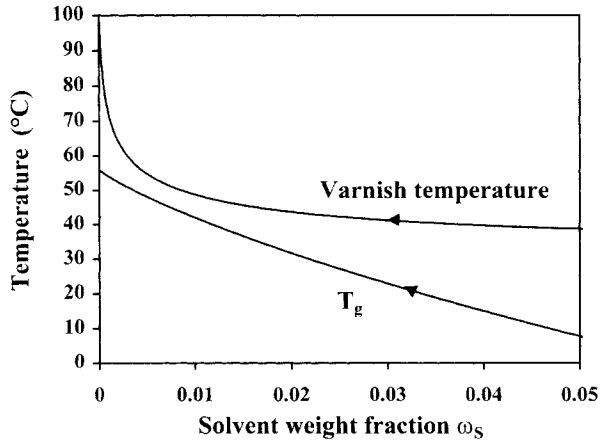

Figure 7. Comparison of film temperature and glass transition temperature.

Kinetics Analysis: Evaporation Experiments in Ambient Air

Due to obvious industrial limitations, it is not possible to get experimental data on the solvent mass evolution inside the dryer. That is why simple evaporation experiments were performed on the same varnish, with continuous recording of mass evolution, in order to compare experimental and simulated kinetics. Unlike for the industrial process using blowing air (forced convection), the exchanges with air in these experiments are mainly diffusive, and new exchange coefficients have been estimated. We will see that the main characteristics of the drying kinetics are the same, that is, the existence of two regimes and the development of important gradient concentration in the layer.

Description of the experiments and estimation of the exchange coefficients

A copolymer solution, about 3 mm thick at the beginning, dries under evaporation at room temperature, without forced

convection. The initial solvent mass fraction is 0.8 (i.e., ES = 0.2), as in the simulation performed in the preceding section. Mass measurements are recorded all along the drying, thanks to a precise balance with a resolution of 10^{-4} g.

The thermal and mass-transfer coefficients have been estimated from the data obtained for pure solvent (MEK) evaporation, without polymers, using the following approximations:

- A 1-D model is still considered. The 2-D effects due to the experimental geometry (the solution container is 37 mm in diameter) are taken into account thanks to the estimated equivalent transfer coefficients.
- The experiments are performed at room temperature, equal to the initial varnish temperature. Because the transfer with air is mainly diffusive, the mass-transfer coefficient h_m is much smaller than in the industrial configuration. As a consequence, the decrease in the varnish temperature due to solvent evaporation is not very important and the assumption of a unique temperature to describe the varnish was maintained.
- Unlike for the industrial configuration, the time of establishment of the permanent regime cannot be neglected. It was taken into account through a time-variable mass-transfer coefficient $h_m(t)$.

The exchange coefficient was obtained in the following way. An initial guess of the estimation was made with the assumption of a purely diffusive transfer of the solvent vapor in air, considering the following boundary and initial conditions: the initial solvent concentration in air is 0. At $t > 0$, the concentration of solvent in air is 0 at a large distance L and constant at the interface. It can be shown that the mass flux is written in the form of a constant plus an infinite sum of exponentials $\exp(-k^2 t D_{\mathrm{MEK/air}}/L^2)$, with $k = 1, 2, \ldots, \infty$, where $D_{\mathrm{MEK/air}}$ is the diffusivity of MEK in air. We took $D_{\mathrm{MEK/air}} = 10^{-5}$ m^2/s and $L = 30$ cm. To take the deviation from the assumption of purely 1-D diffusion into account, a simple estimation procedure was performed: it consists of adjusting the coefficients of the exponential terms in order to fit the experimental data. A very good agreement was obtained with $k = 3$ exponential terms, with the following values:

$$h_m(t) = [1 + 0.406\exp(-t/10^3) + 0.255\exp(-4t/10^3) + 0.298\exp(-9t/10^3)] \times 9.5 \times 10^{-4} \text{ m/s},$$

where t is expressed in seconds:

$$h_{th}^{\mathrm{sup}} = 2.73 \text{ W/m}^2\cdot\text{°C}, \qquad h_{th}^{\mathrm{inf}} = 100 \text{ W/m}^2\cdot\text{°C},$$

where h_{th}^{sup} and h_{th}^{inf} are estimated, respectively, from the thermal transfer in the air and from the thermal contact between the varnish container and the balance plate.

Results

Figure 9 gives experimental and simulated evolutions of the evaporation flux for different values of the diffusion coefficient. Note that, since these experiments were performed at room temperature, the assumption of pure Fickian diffusion ($T > T_g$) is not valid during the whole horizon: for $t > 6{,}500$ s, the difference between the varnish temperature and its glass transition temperature becomes less than 10°C.

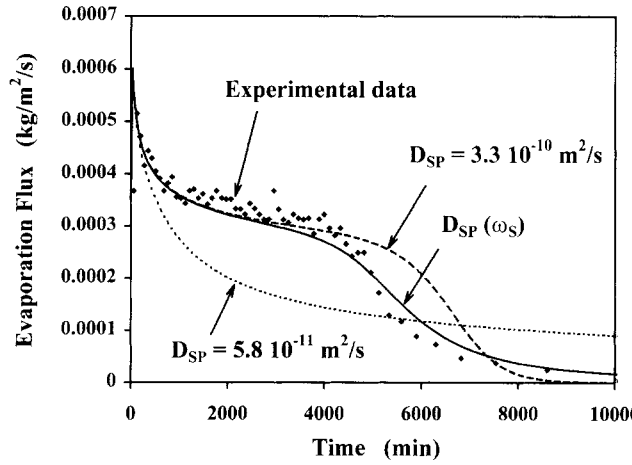

Figure 9. Evaporation flux: experimental vs. simulated flux for different laws of variation of the diffusion coefficient.

The experimental data show again the two regimes described in the preceding section, the transition occurring for $t_1 \simeq 4{,}500$ s. The length of the first regime is about 10^4 times larger than in the industrial configuration, in agreement with that expected. Indeed, in the first regime, where the kinetics is controlled by evaporation in air, that is, by the mass-transfer coefficient, h_m, it can be shown from Eq. 2 that the ratio $h_m t_1/e_0$ should be nearly the same in the industrial and in the laboratory configurations (given that $(P_{VS})_{\mathrm{interface}}$ has the same order of magnitude since temperature is similar in both cases). Consequently this factor, 10^4, was not unexpected.

The solid line in Figure 9 corresponds to the simulation obtained with $\chi = 0.5$, and the diffusion coefficient given in (Hwang and Cohen, 1984) (Figure 3). As can be seen, the agreement is good and the main characteristics of the kinetics are well reproduced. It should be emphasized that a perfect fit between the experimental and simulated curves was not expected. Indeed, as with many industrial varnishes, the varnish studied in this article is a blend of several copolymers. As mentioned previously, physicochemical parameters (as diffusion coefficient or interaction parameter) are not available for complex blends, so that approximate values had to be used in the simulation presented earlier.

The two other simulations reported in Figure 9 were done using a constant diffusion coefficient: $D_{SP} = 3.3 \times 10^{-10}$ m^2/s, corresponding to the maximal value of $D_{SP}(\omega_S)$, and $D_{SP} = 5.8 \times 10^{-11}$ m^2/s corresponding to the value $D_{SP}(\omega_S = 0.25)$ (see Figure 3). As expected, these two coefficients do not succeed in restoring the drying evolution: in the first case ($D_{SP} = 3.3 \times 10^{-10}$ m^2/s), the concentration gradients in the layer are not important, so the evaporation flux is driven mainly by the decreasing of partial pressure vapor as the solvent concentration decreases. On the contrary, for $D_{SP} = 5.8 \times 10^{-11}$ m^2/s, the evaporation slows down from the very beginning, due to a large concentration gradient and the rapid decreasing of concentration near the interface. Finally, we observed that the simulation of these experiments shows a large sensitivity to the choice of the physicochemical parameters. This validates the order of magnitude of the coefficients used in the previous section.

Conclusion

In this article, a complete theoretical description of a drying process was proposed, taking into account the exchange with drying air, the solvent diffusion through the polymer layer, and the coupled heat and mass transfers. The influence of both exchange coefficients and physicochemical properties of the solution have been investigated. This model was developed with the assumption of Fickian diffusion (rubbery state). The comparison at each point of the varnish temperature with its glass transition temperature allows us to check the validity of this assumption.

The kinetics shows two regimes, and the transition between these two regimes is characterized by the development of a very important concentration gradient due to the hypodiffusive behavior of polymer solutions. The results obtained for parameters corresponding to typical industrial conditions were confirmed by the comparison of the proposed model with experimental data obtained from laboratory experiments.

It should be emphasized that the solution properties for a very weak concentration of solvent ($\omega_S \to 0$), which are still not well understood, are found to be of great importance in analyzing the kinetics. In particular, the introduction of anomalous diffusion in the simulation should be one of the developments of the proposed study and would give a better description of the end of the drying.

Acknowledgments

This work was supported by Pechiney Emballage Flexible Europe, France.

Literature Cited

Benard, C., C. Bouchard, B. Guerrier, and G. Zwyngedauw, "Simulation d'un Procédé de Séchage des Vernis," *Proc. Congrès SFT*, Paris, France, p. 358 (1994).

Berens, A. R., "Transport of Organic Vapors and Liquids in Poly(Vinyl Chloride)," *Makromol. Chem., Macromol. Symp.*, **29**, 95 (1989).

Billovits, G. F., and C. J. Durning, "Linear Viscoelastic Diffusion in the Poly(styrene)-Ethylbenzene System: Differential Sorption Experiments," *Macromol.*, **26**, 6927 (1993).

Billovits, G. F., and C. J. Durning, "Linear Viscoelastic Diffusion in the Poly(styrene)-Ethylbenzene System: Comparison Between Theory and Experiment," *Macromol.*, **27**, 7630 (1994).

Bird, R. B., W. E. Stewart, and E. N. Lightfoot, *Transport Phenomena*, Wiley, New York (1960).

Blum, F. D., and S. Pickup, "Solvent Self-Diffusion in Polystyrene-Solvent Systems," *J. Coatings Technol.*, **59**(753), 53 (1987).

Brandrup, J., and E. H. Immergut, *Polymer Handbook*, Wiley Interscience, New York (1989).

Cairncross, R. A., S. Jeyadev, R. S. Dunham, K. Evans, L. F. Francis, and L. E. Scriven, "Modeling and Design of an Industrial Dryer with Convective and Radiant Heating," *J. Appl. Polym. Sci.*, **58**, 1279 (1995).

Caroli, B., C. Caroli, and B. Roulet, "Instabilities of Planar Solidification Fronts," *Instabilities of Planar Solidification Fronts of: Solids Far from Equilibrium*, C. Godreche, ed., Cambridge Univ. Press, New York (1992).

Chow, T. S., "Molecular Interpretation of the Glass Transition Temperature of Polymer-Diluent Systems," *Macromol.*, **13**, 362 (1980).

Crank, J., *Free and Moving Boundary Problems*, Clarendon Press, Oxford (1988).

DeGennes, P. G., *Scaling Concepts in Polymer Physics*, Cornell Univ. Press, Ithaca, NY (1979).

Duda, J. L., Y. C. Ni, and J. S. Vrentas, "Toluene Diffusion in Molten Polystyrene," *J. Appl. Poly. Sci.*, **23**, 947 (1979).

Durning, C. J., and M. Tabor, "Mutual Diffusion in Concentrated Polymer Solutions under a Small Driving Force," *Macromol.*, **19**, 2220 (1986).

Edwards, D. A., and D. S. Cohen, "The Effect of a Changing Diffusion Coefficient in Super-Case II Polymer-Penetrant Systems," *IMA J. Appl. Math.*, **55**, 49 (1995a).

Edwards, D. A., and D. S. Cohen, "A Mathematical Model for a Dissolving Polymer," *AIChE J.*, **41**, 2345 (1995b).

Flory, P. J., *Principles of Polymer Chemistry*, Cornell Univ. Press, Ithaca, NY (1953).

Gall, T. P., R. C. Lasky, and E. J. Kramer, "Case 2 Diffusion: Effect of Solvent Molecule Size," *Polymer*, **31**, 1491 (1990).

Gardon, R., and J. C. Akfirat, "Heat Transfer Characteristics of Impingement Two-Dimensional Air Jets," *J. Heat Transfer*, **88**, 101 (1966).

Hwang, D., and C. Cohen, "Diffusion and Relaxation in Polymer-Solvent Systems. 1. Poly(n-butyl methacrylate)/Methyl Ethyl Ketone," *Macromol.*, **17**, 1679 (1984).

Krantz, W. B., R. J. Ray, R. L. Sani, and K. J. Gleason, "Theoretical Study of the Transport Processes Occurring during the Evaporation Step in Asymmetric Membrane Casting," *J. Memb. Sci.*, **29**, 11 (1986).

Leibler, L., and K. Sekimoto, "On the Sorption of Gases and Liquids in Glassy Polymers," *Macromol.*, **26**, 6937 (1993).

Lodge, T. P., J. A. Lee, and T. S. Frick, "Probe Diffusion in Poly(Vinyl Acetate)/Toluene Solutions," *J. Poly. Sci. Part B Poly. Phys.*, **28**, 2607 (1990).

Martin, H., "Heat and Mass Transfer Between Impinging Gas Jets and Solid Surfaces," *Adv. Heat Transfer, New York*, **13**, 1 (1977).

Neogi, P., *Diffusion in Polymers*, Dekker, New York (1996).

Rossi, G., P. A. Pincus, and P.-G. De Gennes, "A Phenomenological Description of Case-2 Diffusion in Polymeric Materials," *Europhys. Lett.*, **32**(5), 391 (1995).

Thomas, N. L., and A. H. Windle, "A Theory of Case 2 Diffusion," *Polymer*, **23**, 529 (1982).

Vrentas, J. S., and C. M. Vrentas, "Drying of Solvent-Coated Polymer Films," *J. Poly. Sci. Part B Poly. Phys.*, **32**, 187 (1994).

Vrentas, J. S., C. M. Jarzebski, and J. L. Duda, "A Deborah Number for Diffusion in Polymer-Solvent Systems," *AIChE J.*, **21**(5), 895 (1977).

Vrentas, J. S., J. L. Duda, and H. C. Ling, "Free-Volume Theories for Self-Diffusion in Polymer-Solvent Systems. I. Conceptual Differences in Theories," *J. Poly. Sci.*, **23**, 275 (1985).

Waggoner, R. A., F. D. Blum, and J. M. D. MacElroy, "Dependence of the Solvent Diffusion Coefficient on Concentration in Polymer Solutions," *Macromol.*, **26**, 6841 (1993).

Manuscript received Oct. 28, 1996, and revision received Dec. 23, 1997.